WALAILAK JOURNAL

MiniReview

# U60 Undulator: An Insertion Device for the Siam Photon Source

**Thananchai DASRI**

*School of Science and Technology, Nong Khai Campus, Khon Kaen University, Nong Khai 43000, Thailand*

**(Corresponding author; e-mail: thananchai_dasri@hotmail.com)**

*Received: 7th February 2011, Revised: 18th April 2011, Accepted: 27th April 2011*

**Abstract**

Properties of insertion device, undulators, for the synchrotron light source are reviewed. Undulators are magnetic devices installed in the storage ring to improve the properties of the synchrotron light. First, the ideal simulated undulator fields will be discussed. Later the simulated fields produced by a defective undulator will be shown. Last, their effects on the stored electron beam are presented. The U60 undulator of the Siam Photon Source is used as an example.

**Keywords:** U60 undulator, undulator field, Siam Photon Source

## Introduction

Synchrotron radiation is the electromagnetic radiation emitted when a charged particle is accelerated, i.e. constrainted to move in curved paths by a magnetic field. The most common synchrotron light source is a bending magnet. However, the new generation of electron storage ring is designed to contain long straight sections for installation of insertion devices. For example the Siam Photon Source (SPS) storage ring has 4 straight sections, each with the length of 5.2 meters, shown in **Figure 1**. Superior characteristics of synchrotron light from insertion devices will enable the SPS to better serve the various research fields. There are 2 classes of insertion device. One is a wiggler and the other is an undulator. This classification is based on the value of the so-called wiggler strength *K*, defined by

$$K = 0.934 B_0 \lambda_u, \quad (1)$$

where $\lambda_u$ is the period length of the magnetic field in cm and $B_0$ is the magnetic peak field in tesla. An undulator has a low *K*, theoretically, $K << 1$ whereas a wiggler has a large *K*, theoretically $K >> 1$.

Undulators consist of a series of dipole magnets with alternating polarity. The central pole with a strong field is used as a source of radiation. Two side poles with a weaker field at the entrance and exit are used for compensation of orbit distortion of electron beam, i.e. to satisfy zero first and second field integrals,

$$I_y(z) = \int_{z'=0}^{z'=z} B_y(z')dz' = 0, \quad (2)$$

$$J_y(z) = \int_{z'=0}^{z'=z} \int_{z''=0}^{z''=z'} B_y(z'')dz''dz' = 0, \quad (3)$$

where $B_y(z)$ is vertical magnetic field along the z-axis.

A soft x-ray undulator named U60 shown in **Figure 2a** is a type installed in the SPS storage ring. It is a planar permanent magnet (PPM) undulator containing 41 magnetic periods, with 60 mm period length. The total length of the undulator was designed to be 2520 mm, which will occupy approximately half the space in one of the straight sections.

Furthermore, undulators consist of magnetic blocks of alternating polarity that repetitively bend the electron beam back and forth. The magnetic structure is designed such that the deflection angle, the angle between electron trajectory and undulator axis is within $\frac{1}{\gamma}$, where $\gamma$ is the relativistic factor. Synchrotron light emitted from each turn adds coherently, resulting in high intensity undulated radiation. The intensity is proportional to the square of the number of periods. In addition, the opening angle at any given wavelength of the radiation is decreased by $\sqrt{N}$, where $N$ is the number of magnetic periods. **Figure 3** shows a series of harmonics of U60 spectrum. The spectrum clearly shows that the flux density, within some specific energy range, produced from the U60 undulator is higher than that from the bending magnet and wavelength shifter. This higher intensity results from the constructive interference of synchrotron light emitted by the electron beam moving through each magnetic pole of the undulator. However, characteristics of synchrotron light from real undulators are different from ideal devices. This fact arises from magnetic field errors of real undulators. [1-5]. Consequently, they perturb the electron beam in the storage ring. Apart from perturbing the orbit the undulator also gives a tune shift of the electron beam in the storage ring. This tune shift arises from both internal characteristic of the undulator itself and the field errors. Too large tune shift can lead to instability of the electron beam. Moreover, the undulator magnetic field may also have nonlinear terms, especially the sextupole term, which may also give rise to instability.

In this paper, some properties of undulator magnets will be reviewed as radiation sources in the electron storage ring. The affect of the undulator magnetic field on the synchrotron light, how it perturbs the electrons in the storage ring and the undulator magnetic fields will be discussed first. Later, the effects on electrons will be reviewed.

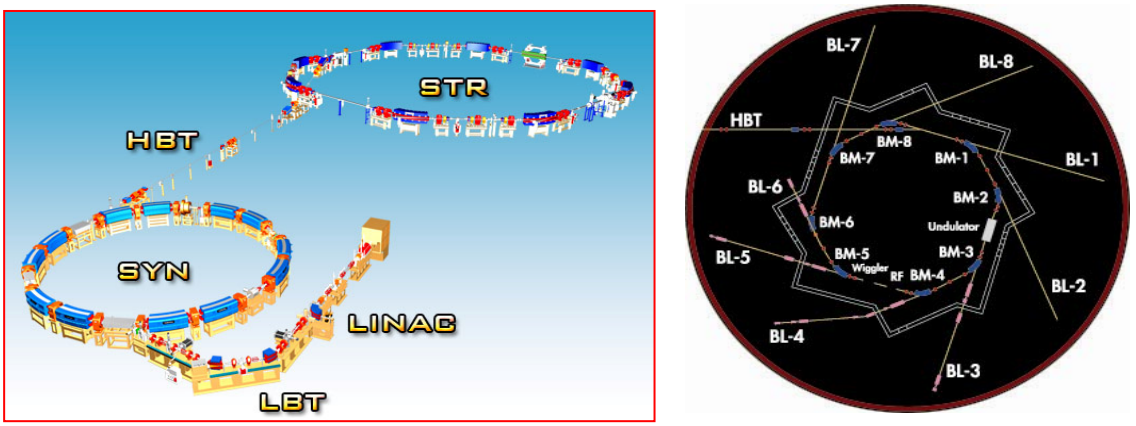


(a) (b)

**Figure 1** (a) The SPS accelerator layout and (b) the SPS electron storage ring that has four straight sections [6].

(a)

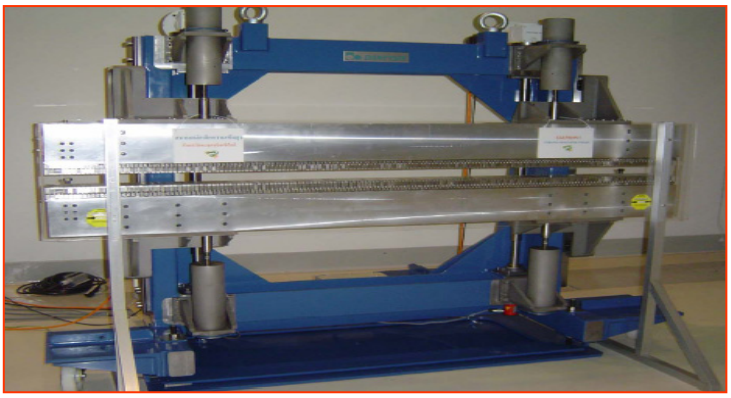

(b)

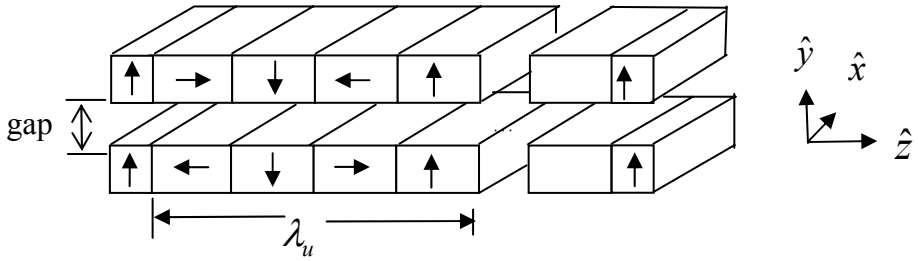


**Figure 2** (a) U60 undulator [7] and (b) a magnetic structure of planar undulator. The arrow in each magnet block indicates the direction of magnetization.

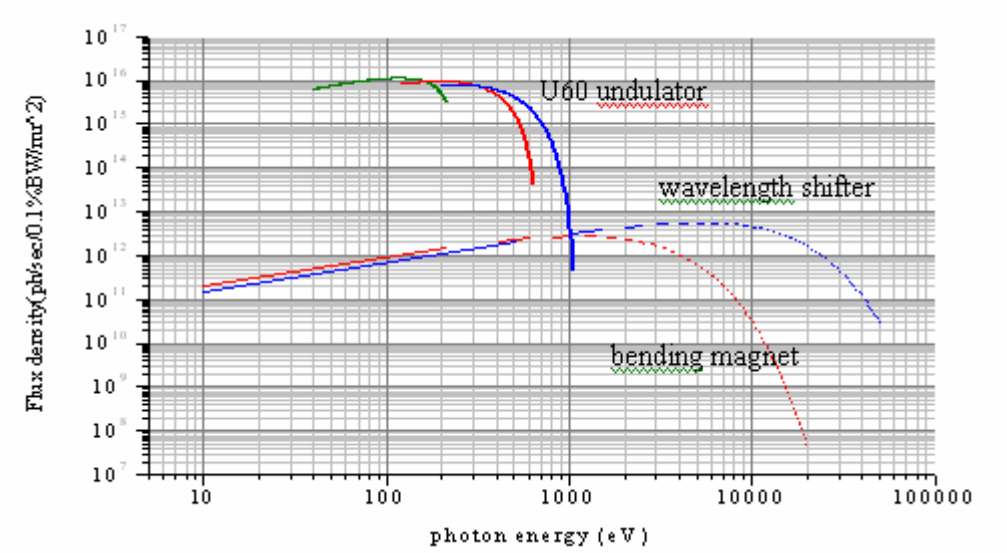


**Figure 3** Flux density as a function of photon energy, up to the 5th harmonic, emitted by a 1.2 GeV electron beam of 100 mA through the U60 undulator, compared with a bending magnet and wavelength shifter spectrum [7].

**Undulator magnetic field**

In this section the undulator magnetic field will be reviewed. A planar undulator is constructed of square magnetic block elements arranged in the Halbach configuration [8]. The two end blocks are half length blocks for end field correction. This is illustrated in **Figure 2b**. The magnetic block with the magnetization $\vec{M}$ and size $X$ , $Y$ and $Z$ is shown in **Figure 4a**. The vertical component of the magnetic field at position ( $x, y, z$ ) produced by such a magnetic block can be calculated by [8-10].

$$\begin{aligned} B_y(x,y,z) = &[b(X,Y,Z) - b(-X,Y,Z) \\ &-b(X,-Y,Z) - b(X,Y,-Z) \\ &+b(-X,-Y,Z) + b(X,-Y,-Z) \\ &-b(-X,Y,-Z) - b(-X,-Y,-Z)]. \end{aligned} \quad (4)$$

By decomposing $\vec{M}$ in the $y$ -component, coefficient $b(x, y, z)$ is given by

$$b(X,Y,Z) = \frac{Br_y}{4\pi}\tan^{-1}\left[\frac{(x-\frac{X}{2})(z-\frac{Z}{2})}{(y-\frac{Y}{2})\left(\sqrt{(\frac{X}{2}-x)^2+(\frac{Y}{2}-y)^2+(\frac{Z}{2}-z)^2}\right)}\right]. \quad (5)$$

Decomposing $\vec{M}$ in the $z$ -component,

$$b(X,Y,Z) = \frac{-Br_z}{4\pi}\ln\left[\frac{X}{2}-x+\sqrt{(x-\frac{X}{2})^2+(y-\frac{Y}{2})^2+(z-\frac{Z}{2})^2}\right]. \quad (6)$$

Similarly, decomposing $\vec{M}$ in the $x$ -component,

$$b(X,Y,Z) = \frac{-Br_x}{4\pi}\ln\left[\frac{Z}{2}-z+\sqrt{(x-\frac{X}{2})^2+(y-\frac{Y}{2})^2+(z-\frac{Z}{2})^2}\right], \quad (7)$$

where $Br_i$ is the remanent field, $i = x, y, z$ , and the origin of the coordinate system is at the center of the block. The undulator field can then be calculated by summing the contributions from each block. The size of the blocks are initially set to a width of $X$ = 46 mm and a height of $Y$ =15 mm[7]. The magnetic block length is determined by the period length, $z = \frac{\lambda_u}{4}$ . The remanent field is fixed at 1.38 T, which is approximately the achievable maximum value for commercially available magnetic blocks.

First, the simulated undulator magnetic field of an ideal device is shown. The ideal planar undulator field in both planes at a gap of 20 mm [7] is illustrated in **Figure 5**. It can be seen that the horizontal field is negligibly small. The vertical magnetic field is sinusoidal in shape. It has 41 full periods. The peak vertical magnetic field is 0.8647 T. By substituting this peak magnetic field and the period length ( $\lambda_u = 6$ cm ) in the equation

$$\varepsilon_1 = \frac{0.950E^2}{(1+\frac{K^2}{2})\lambda_u}, \quad (8)$$

the fundamental photon energy $\varepsilon_1$ is obtained, i.e. $\varepsilon_1$ = 17.88 eV. For the SPS, the photon energy $E$ is 1.2 GeV.

Another undulator magnetic field is the magnetic field produced by the defective undulator. The magnetic fields are generated by variation of the magnetization of the magnetic blocks. Random errors of the magnitude and direction of the magnetization vector in each magnetic block, shown in **Figure 4b**, are simulated. Two sets of random variation are performed to show effects of the errors. The first set is 1 % deviation of the magnetization strength from a nominal value, $\left|\frac{\Delta B_r}{B_r}\right|$, $\leq 1\%$ and 1 degree deviation of the magnetization direction from a nominal magnetization axis, $|\Delta\theta| \leq 1^0$ . The second set is $\left|\frac{\Delta B_r}{B_r}\right| \leq 5\%$ and $|\Delta\theta| \leq 5^0$ .

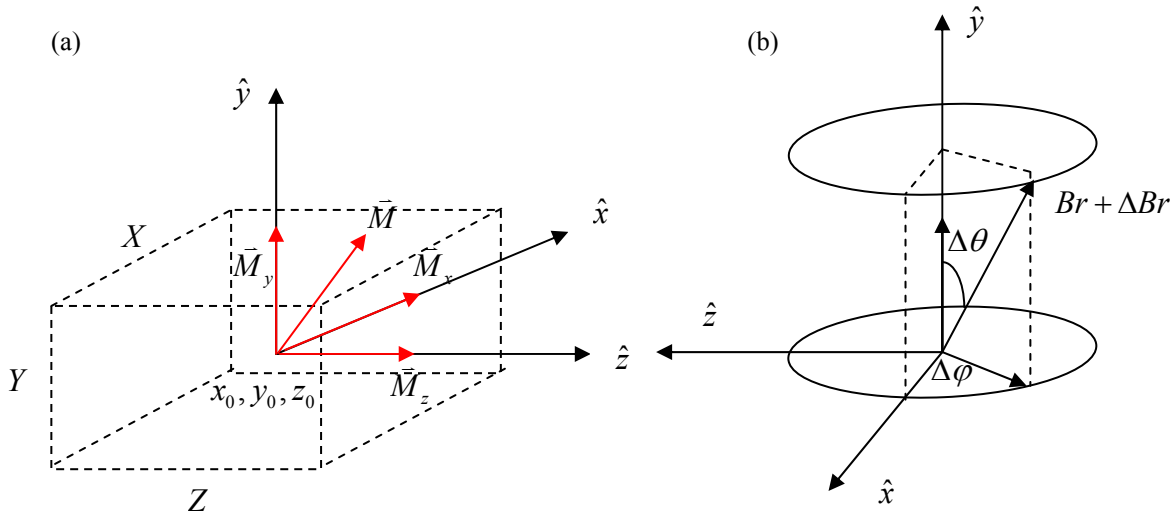


**Figure 4** (a) The permanent rectangular magnet with magnetization in an arbitrary direction. (b) the magnetization vector of a magnetic block.

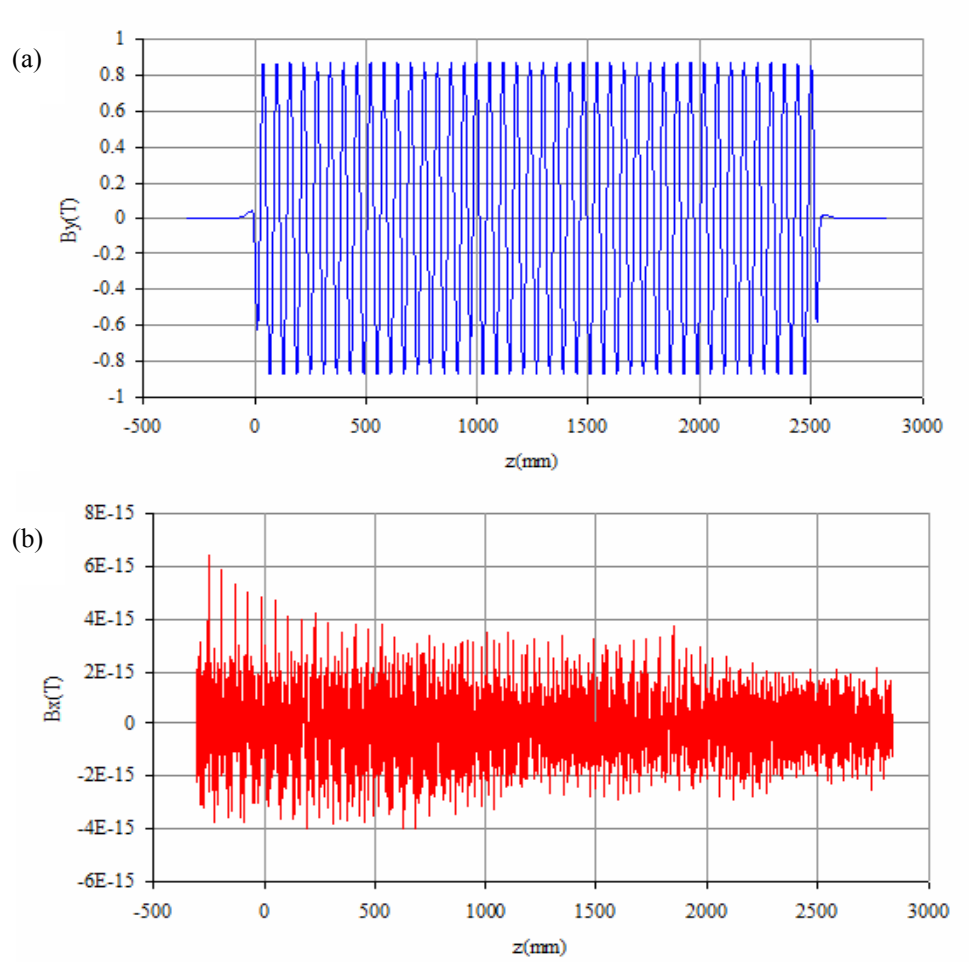


**Figure 5** Simulated on-axis U60 field at 20 mm gap; (a) vertical field (b) horizontal field [7].

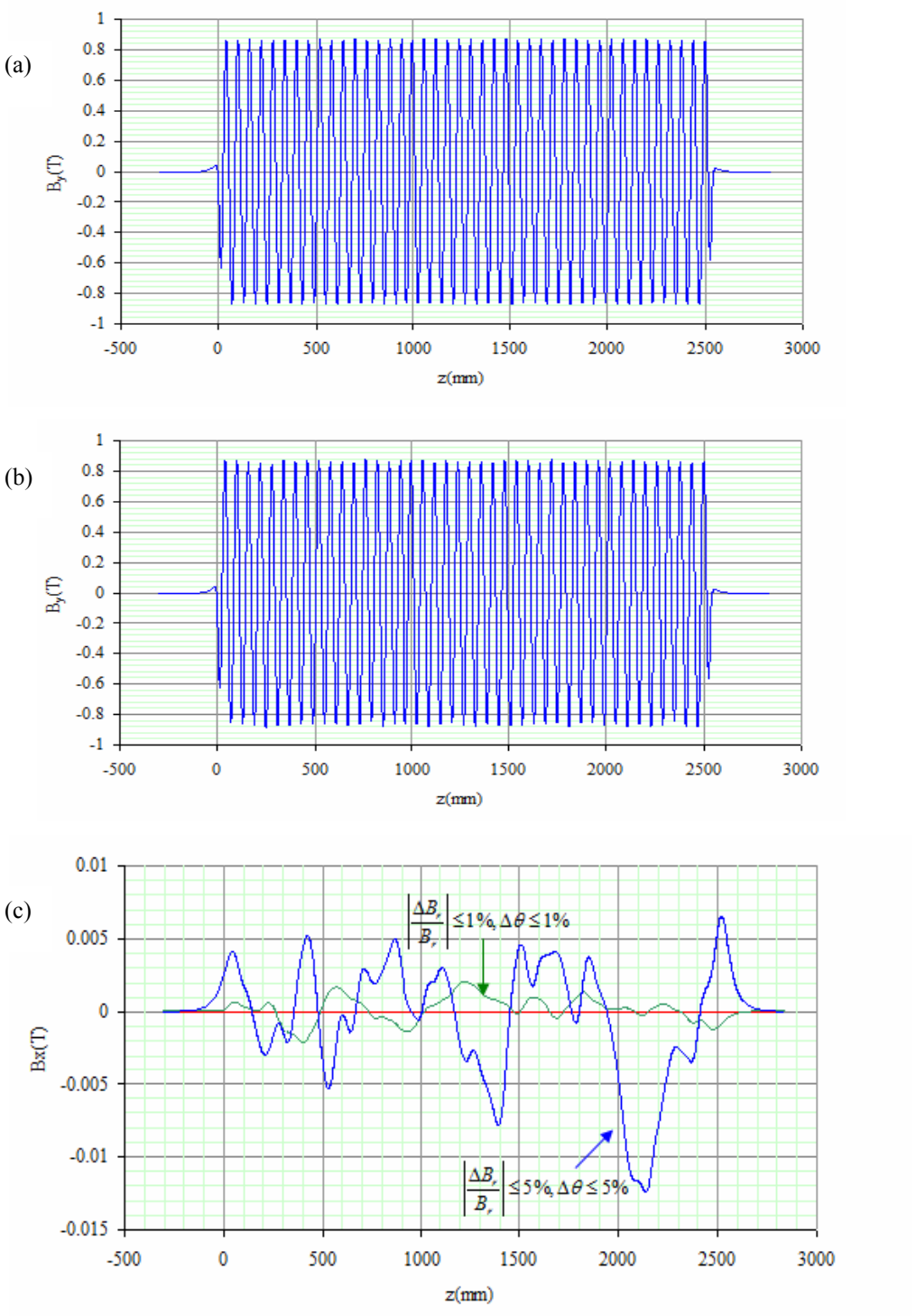


**Figure 6** The simulated vertical fields for the cases: (a) $\left|\frac{\Delta B_r}{B_r}\right| \le 1\%$, $|\Delta\theta| \le 1^0$ and (b) $\left|\frac{\Delta B_r}{B_r}\right| \le 5\%$, $|\Delta\theta| \le 5^0$ and (c) is the simulated horizontal fields [7].

**Electron trajectory perturbation**

This section reviews the effects on an electron moving inside the device. **Figure 7a** is the simulated electron trajectory due to the ideal fields in **Figure 5**. It is clear that an electron will move only on the horizontal plane. In this case the emitted synchrotron light has a higher photon density. The obtained synchrotron light has linear polarization. However, there is an error in the undulator. The undulator will produce a defective field such as the field in **Figure 6**. Thus, the electron beam will move in both planes. **Figure 7b** shows the simulated electron beam trajectory. At the exit of the undulator, the electron is kicked out of the axis with an orbit deviation of 154.87 and 2148.38 $\mu$m for the first and second error sets, respectively [7]. Considering the phase error, the rms phase errors are generated with the values of 1.98° and 16.94° for the first and second error sets, respectively. The phase error affects the quality of the undulator radiation [3,4,11]. The quality of the undulator radiation will be rapidly reduced when the phase error is increased. The photon flux obtained will be more than 90 % of the ideal undulator if the phase error is approximately 1°. So, the maximum $\left|\frac{\Delta B_r}{B_r}\right|$ and $|\Delta\theta|$ should be respectively less than 1% and 1°.

(a)

(b)

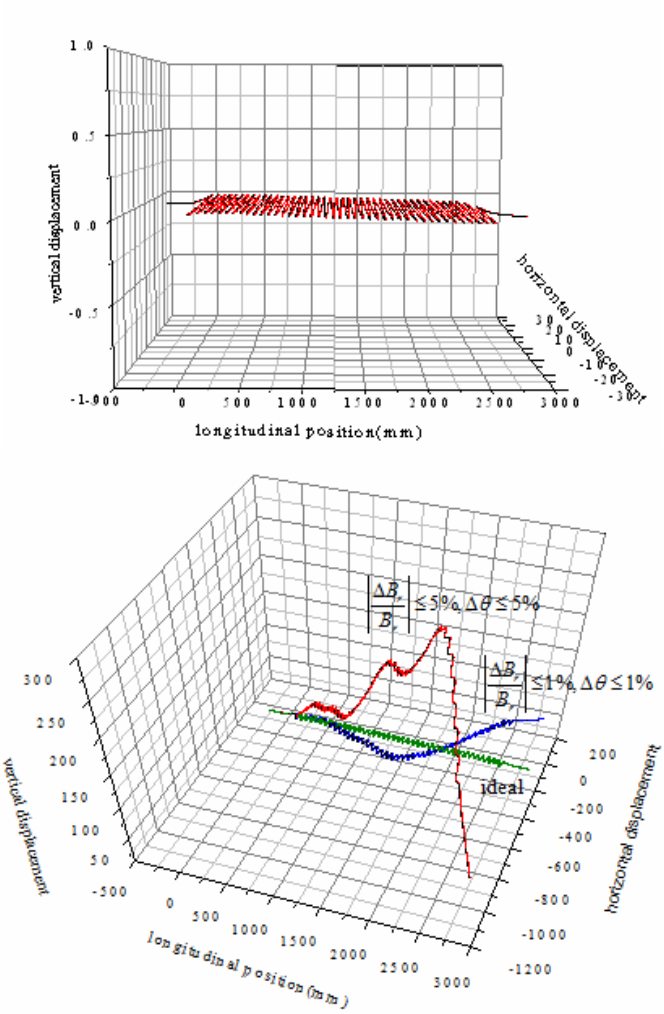


**Figure 7** The calculated trajectory of an electron in (a) the ideal undulator and (b) an undulator with field error [7].

**Summary**

In this paper, some properties of undulators were reviewed. The U60 undulator of the Siam Photon Source is used as an example. First, the magnetic characteristics of an ideal device were illustrated. It can be seen that only a vertical field is produced. Later, the magnetic field errors generated by variation of the magnetization of the magnetic blocks were discussed. It can be seen that both vertical and horizontal fields are produced. Finally, the effects of magnetic fields on the electron beam were also reviewed. It is clear that the magnetic field errors generate a significant horizontal field. The electron therefore orbits in both planes. This effect makes the properties of the synchrotron light decrease.

**Acknowledgements**

I am grateful to Asst. Prof. Dr. Supagorn Rugmai, my Ph.D. thesis advisor for his valuable advice, kindness, and suggestions about the basic theory of insertion devices and synchrotron light sources.

**References**

[1] BL Bobbs, G Rakowsky, P Kennedy, RA Cover and D Slater. In search of a meaningful field-error specification for wiggler. *Nucl. Instrum. Meth.* 1990; **296**, 574-8.

[2] EE Alp and PJ Viccaro. The effect of random field errors on the radiation spectra of selected APS undulators. *Nucl. Instrum. Meth. A* 1988; **266**, 116-9.

[3] BM Kincaid. Random errors in undulators and their effects on radiation spectrum. *J. Opt. Soc. Am. B* 1985; **2**, 1294-306.

[4] BM Kincaid. Analysis of field errors in existing undulators. *Nucl. Instrum. Meth. A* 1990; **291**, 363-70.

[5] RP Walker. Interference effects in undulator and wiggler radiation source. *Nucl. Instrum. Meth. A* 1993; **335**, 328-37.

[6] Synchrotron Light Research Institute Available at: http://www.slri.or.th, accessed March 2011.

[7] T Dasri. 2008, Characterization of soft x-ray undulator for the Siam Photon Source, Ph. D. Dissertation. Suranaree University of Technology, Nakorn Ratchasima, Thailand.

[8] K Halbach. Physical and optical properties of rare earth cobalt magnets. *Nucl. Instrum. Meth*. 1981; **187**, 109-17.

[9] JM Ortega, C Bazin, DAG Deacon, C Depautex and P Elleaume. Realization of the permanent magnet undulator NOEL. *Nucl. Instrum. Meth.* 1983; **206**, 281-8.

[10] G Isoyama. Simulation of a magnetic field correction scheme for Halbach-type undulator. *Rev. Sci. Instrum.* 1989; **60**, 1826-9.

[11] B Diviacco and R P Walker. Recent advances in undulator performance optimization. *Nucl. Instrum. Meth. A* 1996; **368**, 522-32.